metals

MDPI

Article

Combustion Synthesis of $MoSi_2$-Al_2O_3 Composites from Thermite-Based Reagents

Chun-Liang Yeh * and Je-An Peng

Department of Aerospace and Systems Engineering, Feng Chia University, Taichung 40724, Taiwan; m0312018@fcu.edu.tw

* Correspondence: clyeh@fcu.edu.tw; Tel.: +886-4-2451-7250 (ext. 3963)

Academic Editor: Khaled Morsi

Received: 15 July 2016; Accepted: 28 September 2016; Published: 30 September 2016

Abstract: Formation of $MoSi_2$–Al_2O_3 composites with a broad range of the $MoSi_2/Al_2O_3$ ratio was conducted by thermite-based combustion synthesis in the SHS mode. The addition of two thermite mixtures composed of MoO_3 + 2Al and $0.6MoO_3$ + $0.6SiO_2$ + 2Al into the Mo–Si reaction systems facilitated self-sustaining combustion and contributed to in situ formation of $MoSi_2$ and Al_2O_3. The samples adopting the former thermite reagent were more exothermic and produced composites with $MoSi_2/Al_2O_3$ from 2.0 to 4.5, beyond which combustion failed to proceed. Because of lower exothermicity of the reactions, the final products with $MoSi_2/Al_2O_3$ from 1.2 to 2.5 were fabricated from the SHS process involving the latter thermite mixture. Combustion temperatures of both reaction systems decreased from about 1640 to 1150 °C with increasing $MoSi_2/Al_2O_3$ proportion, which led to a phase transition of $MoSi_2$. It was found that the dominant silicide was β-$MoSi_2$ when the combustion temperature of the synthesis reaction exceeded 1550 °C and shifted to α-$MoSi_2$ as the combustion temperature fell below 1320 °C. The results of this study showed an energy-efficient fabrication route to tailor the phase and content of $MoSi_2$ in the $MoSi_2$–Al_2O_3 composite.

Keywords: self-propagating high-temperature synthesis (SHS); thermite reaction; $MoSi_2$; Al_2O_3; combustion temperature

1. Introduction

Silicides of many transition metals (typically in the IVb, Vb, and VIb groups) are promising candidate materials for high-temperature structural applications, due to their high melting point, low density, high thermal conductivity, and excellent oxidation and corrosion resistance at elevated temperatures [1,2]. A variety of processing techniques, often with two or more in combination, including arc-melting and casting, mechanical alloying, hot pressing, reaction sintering, spark plasma sintering, combustion synthesis, and solid-state displacement reactions have been employed to fabricate transition metal silicides and composites on their basis [3–5]. Among these methods, combustion synthesis in the mode of self-propagating high-temperature synthesis (SHS) takes advantage of the highly exothermic reaction, and hence, has the merits of low energy requirement, short processing time, simplicity, high productivity, and a structural and functional diversity of final products [6–8].

Molybdenum disilicide ($MoSi_2$) is one of the intermetallic silicides with broad applications for constructing combustion chamber parts, missile nozzles, diesel engine glow plugs, and industrial gas burners [9]. In microelectronic devices, $MoSi_2$ thin layers are used as interconnections and contacts [9]. Moreover, the addition of a metallic phase or ceramic compound contributed to an improvement in the creep resistance, fracture toughness, and high-temperature strength of $MoSi_2$. Studies have been performed on many reinforcements, such as Al, W, Cu, SiC, Si_3N_4, ZrB_2, and Al_2O_3 [10–18]. The incorporation of Al_2O_3 or Si_3N_4 to $MoSi_2$ has received particular attention due to excellent

thermal stability and a close match of their thermal expansion coefficients [15–18]. Preparation of the $MoSi_2$–Si_3N_4 composites was investigated by Manukyan et al. [17,18] using molten salt-assisted combustion synthesis, in which a series of experiments adopting the Mo–5Si–0.5NaCl–$m$$Si_3N_4$ ($0.7 \leq m \leq 1.65$) samples was conducted in nitrogen from 1 to 5 MPa. NaCl acted as an inert diluent to control the combustion temperature and aided in transportation of the reactant species. The products obtained at nitrogen pressures higher than 3 MPa were composed of $MoSi_2$, β-Si_3N_4 and a small amount of α-Si_3N_4.

Preparation of transition metal silicides of the Ti–Si, Zr–Si, Nb–Si, Ta–Si, and Mo–Si binary systems was widely studied by the classical SHS method using elemental powder compacts of their corresponding stoichoimetries [19–24]. It should be noted that a preheating temperature of 300 °C was required to establish a planar self-propagating combustion wave for combustion synthesis of $NbSi_2$ and $TaSi_2$ [21,22], and 200 °C for the elemental powder compact of Mo:Si = 1:2 [23]. When combined with thermite reactions using Al as the reducing agent, combustion synthesis represents an in situ approach to preparing intermetallic and ceramic composites reinforced by Al_2O_3 [25]. Moreover, aluminothermic reduction of metal oxides is thermally beneficial for the SHS process. This study takes advantage of aluminothermic reduction of MoO_3 to obtain Mo, Al_2O_3, and a large amount of heat for fabricating the $MoSi_2$–Al_2O_3 composite through self-sustaining combustion. It is useful to point out another energy-saving route to obtain elemental Mo was direct reduction of ammonium molybdate tetrahydrate by a mixture of Zn and Mg [26].

The objective of this study was to fabricate the $MoSi_2$–Al_2O_3 composite with a broad range of the phase composition by thermite-based combustion synthesis. Fabrication of the $MoSi_2$–Al_2O_3 composites with different composition ratios is to achieve potential for tailoring material properties to meet the demands of different applications. For example, the increase of $MoSi_2$ enlarges the thermal conductivity and heat capacity of the composite. Fracture toughness and flexural strength are improved as the content of Al_2O_3 increases. Two thermite mixtures, Al–MoO_3 and Al–MoO_3–SiO_2, were adopted and integrated into the Mo–Si reaction system. The synthesis reaction was conducted with no prior heating on the specimen and the effect of sample stoichiometries was studied on the flame-front velocity, combustion temperature, and phase constituents of the final products.

2. Materials and Methods

The starting materials of this study included Mo (Strem Chemicals, Newburyport, MA, USA, <45 μm, 99.9%), Si (Strem Chemicals, <45 μm, 99.5%), Al (Showa Chemical Co., Tokyo, Japan, <45 μm, 99.9%), MoO_3 (Acros Organics, Pittsburgh, PA, USA, 99.5%), and SiO_2 (Strem Chemicals, 99%). Two thermite reagents were prepared to mix with Mo and Si powders. One combines MoO_3 with the reductant Al at a molar ratio of MoO_3:Al = 1:2. The other employs two metal oxides, MoO_3 and SiO_2, in a proportion of MoO_3:SiO_2:Al = 0.6:0.6:2. Reactions (1) and (2) represent two combustion systems with different thermite mixtures for the production of the $MoSi_2$–Al_2O_3 composites.

$$(x-1)\mathrm{Mo} + (2x)\mathrm{Si} + \mathrm{MoO_3} + 2\mathrm{Al} \rightarrow x\mathrm{MoSi_2} + \mathrm{Al_2O_3} \quad (1)$$

$$(y-0.6)\mathrm{Mo} + (2y-0.6)\mathrm{Si} + 0.6\mathrm{MoO_3} + 0.6\mathrm{SiO_2} + 2\mathrm{Al} \rightarrow y\mathrm{MoSi_2} + \mathrm{Al_2O_3} \quad (2)$$

where the stoichiometric coefficients, x and y, signify the number of mole of $MoSi_2$ formed in the composite containing 1 mole of Al_2O_3 from Reactions (1) and (2), respectively. The values of x and y also represent the molar ratio of $MoSi_2/Al_2O_3$ of the composite. The thermite reaction of MoO_3 + 2Al is extremely exothermic with $\Delta H = -930.7$ kJ and $T_{ad} = 4280$ K [27]. Based upon the heat of formation of $MoSi_2$ ($\Delta H_f = -131.4$ kJ/mol), $T_{ad} = 1770$ K is obtained for the Mo + 2Si reaction [27]. Therefore, the addition of Mo and Si into the thermite mixture had a dilution effect on combustion. In this study, Reaction (1) was conducted with x varying from 2.0 to 4.5, within which stable and self-sustaining combustion was attained. For Reaction (1) with $x < 2.0$, it was difficult to recover the end product because violent combustion accompanying massive melting of the sample

occurred. In contrast, combustion ceased to proceed in Reaction (1) with $x > 4.5$ due to insufficient reaction exothermicity.

For Reaction (2), co-reduction of MoO_3 and SiO_2 by Al was carried out. Despite weaker reaction exothermicity compared with the WO_3 + 2Al reagent, the $0.6WO_3 + 0.6SiO_2$ + 2Al thermite mixture with $\Delta H = -683.7$ kJ and $T_{ad} = 3150$ K [27] is thermally adequate to initiate Reaction (2). The steady self-sustaining combustion for Reaction (2) was found in the range of $1.2 \leq y \leq 2.5$. A combination of Reaction (1) with $2.0 \leq x \leq 4.5$ and Reaction (2) with $1.2 \leq y \leq 2.5$ broadens the $MoSi_2/Al_2O_3$ ratio from 1.2 to 4.5 for the composites. Formation of the $MoSi_2$–Al_2O_3 composite through combustion synthesis involving aluminothermic reduction proceeds in consecutive stages. Reduction of MoO_3 by Al to produce Mo and Al_2O_3 is believed to be the initiation step, followed by aluminothermic reduction of SiO_2 in the case of Reaction (2). Thereupon, $MoSi_2$ is formed from the interaction of Mo and Si.

The reactant powders were well mixed and compressed into cylindrical test specimens with 7 mm in diameter, 12 mm in length, and a relative density of 60%. The SHS reaction was conducted under high-purity (99.99%) argon of 0.15 MPa. The combustion wave velocity (V_f) was precisely determined from the time series of recorded combustion images. The combustion temperature (T_c) of the sample was measured by a fine-wire (125 μm) Pt/Pt-13%Rh thermocouple attached on the sample surface. The synthesized products were analyzed by X-Ray Diffraction (XRD) to identify the phase composition. Details of the experimental methods were reported elsewhere [28].

3. Results and Discussion

3.1. Combustion Front Velocity and Combustion Temperature

Two typical combustion sequences are illustrated in Figure 1a,b, which are respectively associated with Reaction (1) of $x = 3.0$ and Reaction (2) of $y = 2.0$. It is evident that for both SHS processes a distinct combustion front forms upon ignition and propagates along the sample compact in a self-sustaining manner. Figure 1a shows a faster combustion wave and a deformed product caused by melting of the sample, implying its higher combustion exothermicity. Serious melting and collapse of the samples were observed in Reaction (1) with $x = 2.0$–3.0, which generated high combustion temperatures because these samples contained single oxide MoO_3 and relatively less amounts of Mo and Si. Moreover, MoO_3 and Al have very low melting points of 795 °C and 660 °C, respectively.

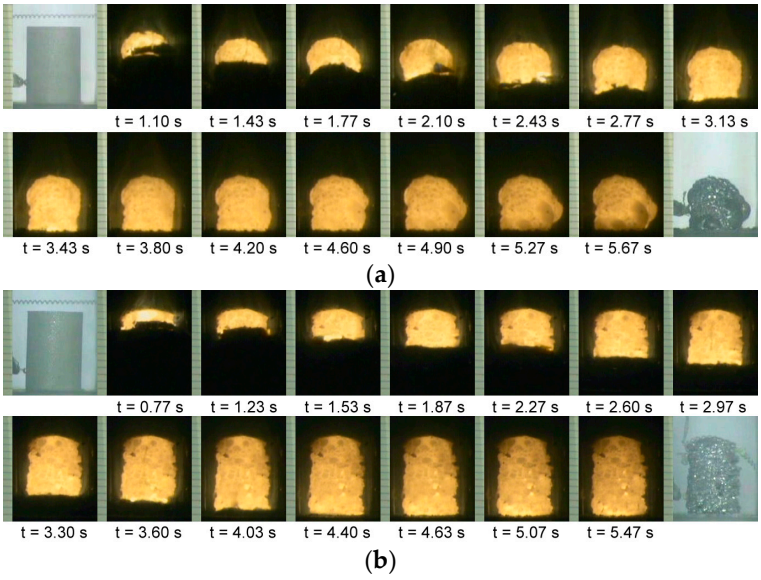

Figure 1. Self-propagating combustion sequences of formation of $MoSi_2$–Al_2O_3 composites: (**a**) Reaction (1) with $x = 3.0$ and (**b**) Reaction (2) with $y = 2.0$.

The melting of the sample was alleviated with increasing content of $MoSi_2$ formed in the composite. The powder compacts of Reaction (2) also experienced lesser melting due to lower reaction enthalpies. As indicated in Figure 1b, only slight sample deformation was observed and the combustion wave was slower than that of Figure 1a.

Figure 2 presents the variations of flame-front propagation velocity (V_f) of Reactions (1) and (2) with respect to their corresponding stoichiometric coefficients, x and y. For Reaction (1), a significant decrease in the combustion wave speed from about 6.5 to 1.7 mm/s was observed with increasing x from 2.0 to 4.5. An increase in the stoichiometric coefficient of the reaction means a larger amount of Mo and Si powders added to the sample. The decrease of combustion front velocity was attributed to the dilution effect of Mo and Si additions, because the formation of $MoSi_2$ was less energetic than aluminothermic reduction of oxide reagents. Similarly, the decrease of the combustion velocity of Reaction (2) from 6.0 mm/s at y = 1.2 to 1.8 mm/s at y = 2.5 is revealed in Figure 2. A comparison between Reactions (1) and (2) at $x = y$ = 2.0 and 2.5 points out that the flame-front velocities of Reaction (1) are much faster than those of Reaction (2). This is most likely caused by the fact that the thermite mixture of MoO_3 + 2Al is more exothermic than that of $0.6MoO_3 + 0.6SiO_2$ + 2Al.

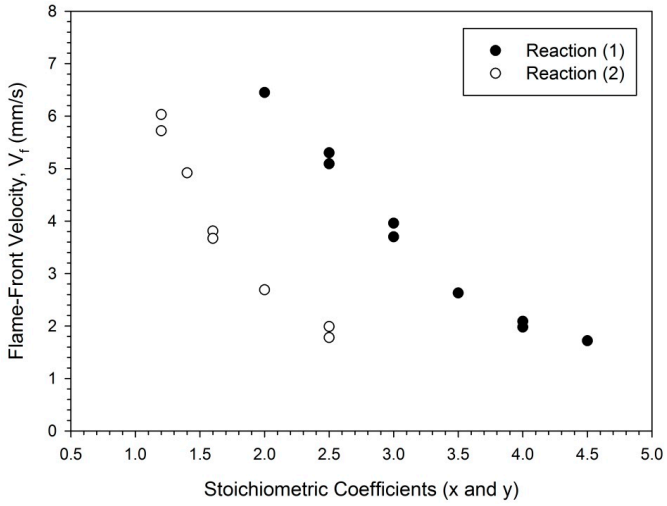

Figure 2. Effects of stoichiometric coefficients of reactions with different thermite reagents on flame-front velocity for formation of $MoSi_2$–Al_2O_3 composites.

Figures 3 and 4 plot combustion temperature profiles measured from the powder compacts of Reactions (1) and (2) with different stoichiometries. The abrupt rise in temperature signifies rapid arrival of the combustion wave and the peak value stands for the reaction front temperature. Figure 3 shows that the combustion front temperature of Reaction (1) decreases from 1645 to 1198 °C as the molar ratio of $MoSi_2/Al_2O_3$ increases from x = 2.0 to 4.5, confirming a decline in the overall reaction exothermicity with Mo and Si additions. As presented in Figure 4, for the samples of Reaction (2) a decrease in the peak combustion temperature from 1587 to 1146 °C was detected with increasing proportion of $MoSi_2/Al_2O_3$ from y = 1.2 to 2.5. A comparison between Figures 3 and 4 verifies that Reaction (1) is more exothermic than Reaction (2). In addition, the temperature profiles of Reaction (1) appear to be broader than those of Reaction (2). This is because the amount of heat generated by Reaction (1) is larger than that generated by Reaction (2). Consequently, the rate of temperature decline behind the combustion front is slower for the sample of Reaction (1). Furthermore, it is useful to note that for Reactions (1) and (2), the composition dependence of the combustion temperature is in agreement with that of combustion wave velocity.

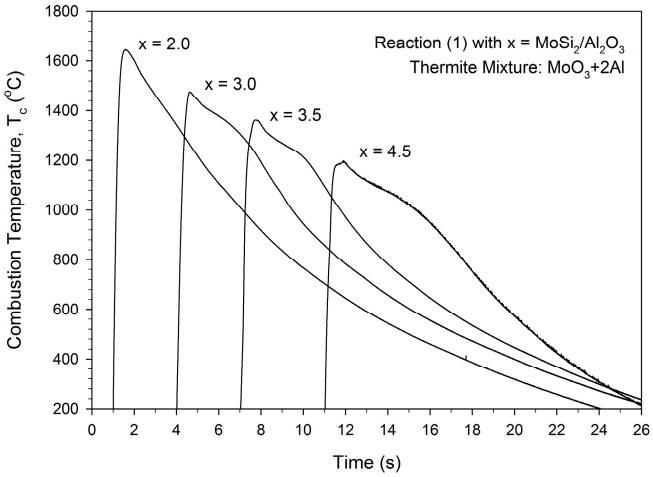

Figure 3. Variation of combustion temperature with $MoSi_2/Al_2O_3$ ratio of composites synthesized by self-propagating high-temperature synthesis (SHS) involving reduction of MoO_3 by Al.

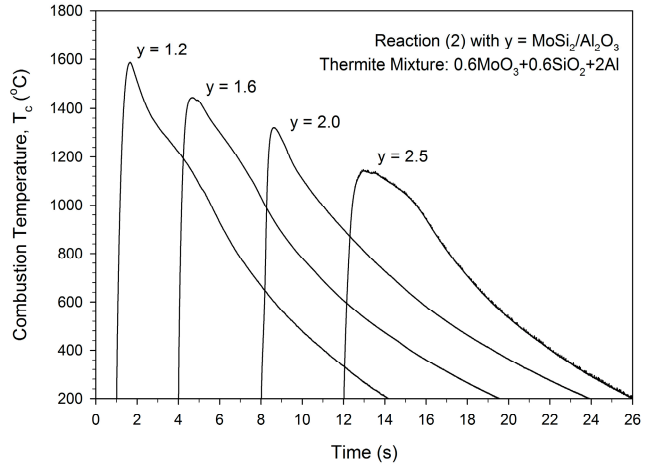

Figure 4. Variation of combustion temperature with $MoSi_2/Al_2O_3$ ratio of composites synthesized by SHS involving co-reduction of MoO_3 and SiO_2 by Al.

3.2. *Phase Constituents of Synthesized Composites*

Figure 5a–c displays the XRD patterns of SHS-produced composites from Reaction (1) with different $MoSi_2/Al_2O_3$ ratios. Formation of both α and β phases of $MoSi_2$ was observed. It is noticed that β-$MoSi_2$ (the high-temperature phase) is the dominant silicide in Figure 5a of x = 2.5, which corresponds to $T_{c,max}$ = 1580 °C. With the increase of the coefficient x, a phase transformation from β-$MoSi_2$ to α-$MoSi_2$ (the low-temperature phase) is shown in Figure 5a–c. The phase change is due probably to the decrease of combustion temperature. As reveals in Figure 5c, the silicide phase is governed by α-$MoSi_2$ in the product with x = 4.0, for which $T_{c,max}$ = 1280 °C. β-$MoSi_2$ is a metastable phase with excellent thermoelectric properties, while α-$MoSi_2$ is a stable phase with a low electric resistance and high oxidation resistance [29]. Formation of β-$MoSi_2$ in the final product could be attributed to the high thermal gradient and rapid cooling rate inherent in the SHS process. Experimental evidence of this study indicates that the as-synthesized composite features β-$MoSi_2$ as the major silicide when the combustion temperature exceeds 1550 °C, whereas α-$MoSi_2$ dominates in the final product with combustion temperature lower than 1320 °C.

In addition, the XRD signature of aluminum silicate rather than Al_2O_3 is indexed in the spectra of Figure 5. Aluminum silicate or called mullite is a solid solution of Al_2O_3 and SiO_2. This verified that, in agreement with the initial hypothesis, Al_2O_3 was produced. Because there was Si in the reaction

system, dissolution of a small amount of Si into Al_2O_3 led to the formation of aluminum silicate in the final product. The EDS analysis of the final product indicated a slightly Si-lean atomic ratio of Mo:Si = 37.73:62.27 for the $MoSi_2$ (Mo:Si = 33.33:66.67) phase. Therefore, the amount of Si dissolved into Al_2O_3 was estimated to be about 6.6 atm %.

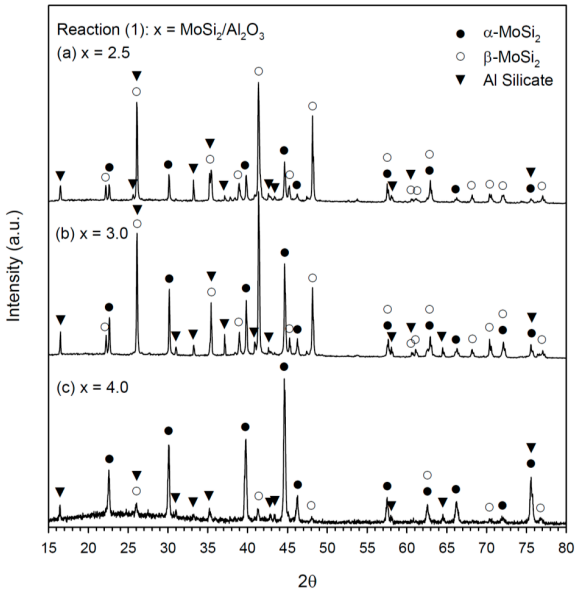

Figure 5. X-Ray Diffraction (XRD) patterns of $MoSi_2$–Al_2O_3 composites synthesized from Reaction (1) with (**a**) x = 2.5; (**b**) x = 3.0; and (**c**) x = 4.0.

Phase constituents of the composites synthesized from Reaction (2) are identical to those from Reaction (1). The dependence of phase evolution of $MoSi_2$ produced by Reaction (2) on combustion temperature is in a manner consistent with that observed in Reaction (1). For the SHS-derived composites of Reaction (2), the silicide of the product of y = 1.2 was dominated by β-$MoSi_2$ because of a high combustion temperature close to 1590 °C, but α-$MoSi_2$ prevailed in the products of y = 2.0 and 2.5 on account of their low combustion temperatures of 1320 and 1146 °C, respectively. The XRD pattern of the composite with y = 2.5 is depicted in Figure 6, which has the same $MoSi_2$ / Al_2O_3 ratio as that shown in Figure 5a. This demonstrates that the phase of $MoSi_2$ is tailorable through the reaction systems with different thermite reagents.

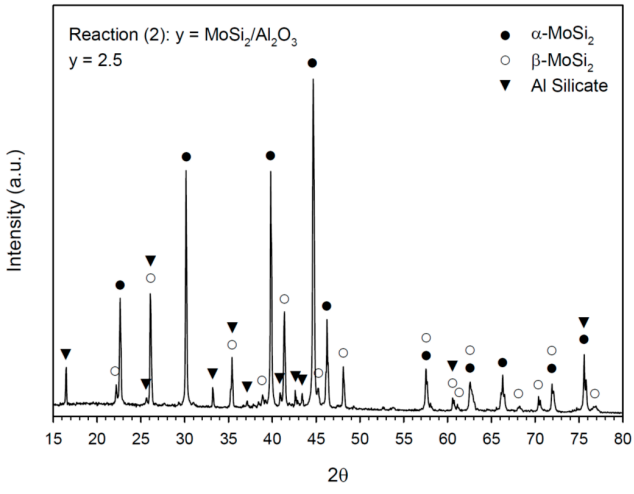

Figure 6. XRD pattern of a $MoSi_2$–Al_2O_3 composite synthesized from Reaction (2) with y = 2.5.

4. Conclusions

The SHS process involving thermite reduction of MoO_3 and SiO_2 was conducted to prepare the in situ $MoSi_2$–Al_2O_3 composites with a broad range of the $MoSi_2/Al_2O_3$ proportion. Two thermite mixtures made up of MoO_3 + 2Al and $0.6MoO_3$ + $0.6SiO_2$ + 2Al were incorporated into the Mo–Si reaction system. Aluminothermic reduction of metal oxides released a large amount of the reaction enthalpy and generated Al_2O_3. The increase of Mo and Si for the production of a higher content of $MoSi_2$ reduced the overall reaction exothermicity and decelerated the combustion wave. The SHS process involving the MoO_3 + 2Al thermite was more exothermic than that containing the $0.6MoO_3$ + $0.6SiO_2$ + 2Al thermite. As a consequence, the former was adopted to produce composites with the $MoSi_2/Al_2O_3$ ratio from 2.0 to 4.5, and the latter aimed for $MoSi_2/Al_2O_3$ from 1.2 to 2.5.

Both reaction systems showed a substantial decrease in combustion temperature from around 1640 to 1150 °C and a reduction in combustion wave velocity from approximately 6.5 to 1.7 mm/s with the increase of the molar ratio of $MoSi_2/Al_2O_3$. The phase of $MoSi_2$ formed in the composite was dependent on the combustion temperature. It was found that β-$MoSi_2$ dominated in the products with combustion temperatures higher than 1550 °C and α-$MoSi_2$ prevailed in those with combustion temperatures below 1320 °C. In addition, dissolution of Si into Al_2O_3 led to the presence of aluminum silicate in the final product.

Acknowledgments: This research was sponsored by the Ministry of Science and Technology, R.O.C. under the grant of MOST 105-2221-E-035-039-MY2. Authors are grateful for the Precision Instrument Support Center of Feng Chia University in providing materials analytical facilities.

Author Contributions: Chun-Liang Yeh conceived and designed the experiments, analyzed the experimental data, supervised the work, and wrote the paper. Je-An Peng performed the SHS experiments and materials analysis.

Conflicts of Interest: The authors declare no conflict of interest. The founding sponsors had no role in the design of the study; in the collection, analyses, or interpretation of data; in the writing of the manuscript, and in the decision to publish the results.

References

1. Meschter, P.J.; Schwartz, D.S. Silicide-matrix materials for high temperature applications. *JOM* **1989**, *41*, 52–55. [CrossRef]
2. Petrovic, J.J.; Vasudevan, A.K. Key developments in high temperature structural silicides. *Mater. Sci. Eng. A* **1999**, *261*, 1–5. [CrossRef]
3. Stoloff, N.S. An overview of powder processing of silicides and their composites. *Mater. Sci. Eng. A* **1999**, *261*, 169–180. [CrossRef]
4. Chen, F.; Xu, J.; Liu, Y.; Cai, L. In situ reactive spark plasma sintering of $WSi_2/MoSi_2$ composites. *Ceram. Int.* **2016**, *42*, 11165–11169. [CrossRef]
5. Reddy, V.; Sonber, J.K.; Sairam, K.; Murthy, T.S.R.C.; Kumar, S.; Nageswara Rao, G.V.S.; Srinivasa Rao, T.; Chakravartty, J.K. Densification and mechanical properties of CrB_2 + $MoSi_2$ based novel composites. *Ceram. Int.* **2015**, *41*, 7611–7617. [CrossRef]
6. Merzhanov, A.G. Combustion and explosion processes in physical chemistry and technology of inorganic materials. *Russ. Chem. Rev.* **2003**, *72*, 289–310. [CrossRef]
7. Liu, G.; Li, J.; Chen, K. Combustion synthesis of refractory and hard materials: A review. *Int. J. Refract. Met. Hard Mater.* **2013**, *39*, 90–102. [CrossRef]
8. Vicario, I.; Poulon-Quintin, A.; Lagos, M.A.; Silvain, J.F. Effect of material and process atmosphere in the preparation of Al–Ti–B grain refiner by SHS. *Metals* **2015**, *5*, 1387–1396. [CrossRef]
9. Yao, Z.; Stiglich, J.; Sudarshan, T.S. Molybdenum silicide based materials and their properties. *J. Mater. Eng. Perform.* **1999**, *8*, 291–304. [CrossRef]
10. Wang, X.; Feng, P.; Akhtar, F.; Wu, J.; Liu, W.; Qiang, Y.; Wang, Z. Effects of tungsten and aluminum additions on the formation of molybdenum disilicide by mechanically-induced self-propagating reaction. *J. Alloy. Compd.* **2010**, *490*, 388–392. [CrossRef]

11. Samadi, M.; Shamanian, M.; Panjepour, M.; Saidi, A.; Abbasi, M.H.; Asgharzadeh, F. Investigation of $MoSi_2$ formation in the presence of copper by self-propagating high-temperature synthesis. *J. Alloy. Compd.* **2008**, *462*, 229–234. [CrossRef]
12. Esmaeily, S.; Kermani, M.; Razavi, M.; Rahimipour, M.R.; Zakeri, M. An investigation on the in situ synthesis-sintering and mechanical properties of $MoSi_2$-*x*SiC composites prepared by spark plasma sintering. *Int. J. Refract. Met. Hard Mater.* **2015**, *48*, 263–271. [CrossRef]
13. Huang, Y.; Lin, J.; Zhang, H. Effect of Si_3N_4 content on microstructures and antioxidant properties of $MoSi_2/Si_3N_4$ composite coatings on Mo substrate. *Ceram. Int.* **2015**, *41*, 13903–13907. [CrossRef]
14. Wang, R.; Li, W. Effects of microstructures and flaw evolution on the fracture strength of ZrB_2–$MoSi_2$ composites under high temperatures. *J. Alloy. Compd.* **2015**, *644*, 582–588. [CrossRef]
15. Wang, J.; Feng, P.; Niu, J.; Guo, R.; Liu, Z.; Akhtar, F. Synthesis, microstructure and properties of $MoSi_2$–5 vol % Al_2O_3 composites. *Ceram. Int.* **2014**, *40*, 16381–16387. [CrossRef]
16. Huang, Z.; Zhou, W.; Tang, X.; Zhu, J. Effects of milling methods on the dielectric and the mechanical properties of hot-pressed sintered $MoSi_2/Al_2O_3$ composites. *J. Alloy. Compd.* **2011**, *509*, 1920–1923. [CrossRef]
17. Manukyan, K.V.; Aydinyan, S.V.; Kirakosyan, K.G.; Kharatyan, S.L.; Blugan, G.; Müller, U.; Kuebler, J. Molten salt-assisted combustion synthesis and characterization of $MoSi_2$ and $MoSi_2$–Si_3N_4 composite powders. *Chem. Eng. J.* **2008**, *143*, 331–336. [CrossRef]
18. Manukyan, K.V.; Kharatyan, S.L.; Blugan, G.; Kocher, P.; Kuebler, J. $MoSi_2$–Si_3N_4 composites: Influence of starting materials and fabrication route on electrical and mechanical properties. *J. Eur. Ceram. Soc.* **2009**, *29*, 2053–2060. [CrossRef]
19. Yeh, C.L.; Chen, W.H.; Hsu, C.C. Formation of titanium silicides Ti_5Si_3 and $TiSi_2$ by self-propagating combustion synthesis. *J. Alloy. Compd.* **2007**, *432*, 90–95. [CrossRef]
20. Bertolino, N.; Anselmi-Tamburini, U.; Maglia, F.; Spinolo, G.; Munir, Z.A. Combustion synthesis of Zr–Si intermetallic compounds. *J. Alloy. Compd.* **1999**, *288*, 238–248. [CrossRef]
21. Yeh, C.L.; Chen, W.H. A comparative study on combustion synthesis of Nb–Si compounds. *J. Alloy. Compd.* **2006**, *425*, 216–222. [CrossRef]
22. Yeh, C.L.; Wang, H.J. A comparative study on combustion synthesis of Ta–Si compounds. *Intermetallics* **2007**, *15*, 1277–1284. [CrossRef]
23. Yeh, C.L.; Chen, W.H. Combustion synthesis of $MoSi_2$ and $MoSi_2$–Mo_5Si_3 composites. *J. Alloy. Compd.* **2007**, *438*, 165–170. [CrossRef]
24. Yeh, C.L.; Chou, C.C.; Hwang, P.W. Experimental and numerical studies on self-propagating high-temperature synthesis of Ta_5Si_3 intermetallics. *Metals* **2015**, *5*, 1580–1590. [CrossRef]
25. Wang, L.L.; Munir, Z.A.; Maximov, Y.M. Thermite reactions: Their utilization in the synthesis and processing of materials. *J. Mater. Sci.* **1993**, *28*, 3693–3708. [CrossRef]
26. Manukyan, K.; Davtyan, D.; Bossert, J.; Kharatyan, S. Direct reduction of ammonium molybdate to elemental molybdenum by combustion reaction. *Chem. Eng. J.* **2011**, *168*, 925–930. [CrossRef]
27. Binnewies, M.; Milke, E. *Thermochemical Data of Elements and Compounds*; Wiley-VCH Verlag GmbH: Weinheim, Germany, 2002.
28. Yeh, C.L.; Lin, J.Z. Combustion synthesis of Cr–Al and Cr–Si intermetallics with Al_2O_3 additions from Cr_2O_3–Al and Cr_2O_3–Al–Si reaction systems. *Intermetallics* **2013**, *33*, 126–133. [CrossRef]
29. Yamada, T.; Yamane, H. Crystal structure and thermoelectric properties of β-$MoSi_2$. *Intermetallics* **2011**, *19*, 908–912. [CrossRef]

© 2016 by the authors; licensee MDPI, Basel, Switzerland. This article is an open access article distributed under the terms and conditions of the Creative Commons Attribution (CC-BY) license (http://creativecommons.org/licenses/by/4.0/).